2

Relativistic model for bremsstrahlung

Bremsstrahlung is one of the simplest available tools for the investigation of the NN interaction, besides elastic scattering. The proposal [40], made long time ago, that it can be used to discriminate between competing models for the strong force has generated a lot of interest over the years, both theoretically and experimentally. In the past years the possibility of such a discrimination between the various existing models for the NN interaction has been under investigation with contradictory results [61, 62]. The study of meson-exchange currents (MEC) and of the Δ isobar has been another motivational source for the study of this reaction, especially in the last two decades since only recently models have accounted for these contributions. They are expected to be important at sufficiently high energies, close to the pion production threshold. Our main concern will be with the relativistic covariant Martinus *et al.* model for bremsstrahlung [52, 63, 65, 66] whose main ingredients will be described in this chapter. Details of other two recent models for $pp\gamma$, the microscopic model of Nakayama *et al.* [49, 64, 67, 68] and the soft-photon theorem [79, 80] based model for virtual nucleon-nucleon bremsstrahlung of Korchin and Scholten [60, 69], will also be presented. Theoretical predictions will be compared with the experimental data for a few selected kinematics of the 190 MeV KVI $pp\gamma$ experiment [57, 58, 81, 82].

2.1 A relativistic covariant model for bremsstrahlung

An important ingredient of the Martinus *et al.* model for bremsstrahlung is the elastic scattering T matrix. It has been obtained from the Fleischer-Tjon one-boson-exchange (OBE) model for the NN interaction [10, 75, 76]. This model is based on a numerical solution of the quasipotential approximation of the Bethe-Salpeter equation introduced by Logunov and Tavkhelidze [83] and Blakenbecler and Sugar [84]. The BSLT equation can be solved in a partial-wave basis [73]. The partial-wave decomposition yields a system of coupled one-dimensional equations for the partial-wave amplitudes. The equation is solved keeping also the contributions from negative-energy states both as intermediate and/or initial (final) states. The latter case is relevant only when one considers the half or the fully off-shell T matrix. The on-shell T matrix was fitted to the np phase shifts of Arndt *et al.* [85] by varying the meson-nucleon coupling constants. The OBE model presented here has been successfully applied to the case of electron-deuteron scattering by Hummel and Tjon [73]. The electromagnetic matrix elements were determined using

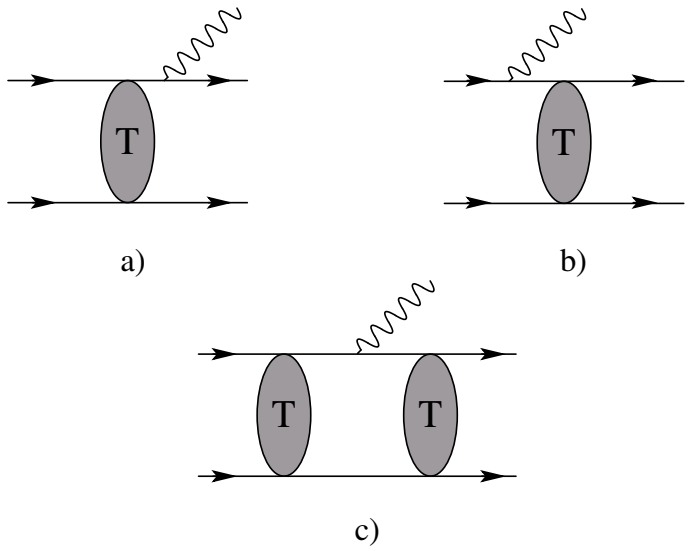

Figure 2.1: Single scattering diagrams contributing to the impulse approximation, (a) and (b), and the rescattering diagram contribution (c). Diagrams in which the photon couples to only one of the protons are shown.

the equal-time approximation [86, 87, 88]. More details about the Fleischer-Tjon OBE model are presented in Chapter 5.

2.1.1 The Martinus *et al.* $pp\gamma$ model

The electromagnetic nuclear current can be split into two parts: the one-body and the two-body current, the former giving the dominant contribution in the energy region we are considering. The invariant amplitude of the bremsstrahlung process is $M_{fi} = \epsilon^\mu \langle f|J_\mu|i\rangle$ with ϵ^μ the polarization four-vector of the emitted photon, while J_μ is the nuclear current, which has its matrix elements given by

$$\begin{aligned}\langle f|J_\mu|i\rangle \;=\; & \langle p', P'|T(p', \tilde{p}; P')S^{(1)}(\tilde{p}, P')\Gamma^{(1)}_\mu(q)|p, P\rangle \\ & + \langle p', P'|\Gamma^{(1)}_\mu(q)S^{(1)}(\tilde{p}', P)T(\tilde{p}', p; P)|p, P\rangle + (1 \leftrightarrow 2) \\ & - i\int \frac{d^4k}{(2\pi)^4}\langle p', P'|T(p', k'; P')S^{(1)}(k', P')\Gamma^{(1)}_\mu(q)S_2(k, P)T(k, p; P)|p, P\rangle\,.\end{aligned} \tag{2.1}$$

The first two terms correspond to what is commonly known as the impulse approximation (IA). They represent the sum of all single-scattering diagrams, when the photon is emitted by one of the external legs. Consistency with the equal-time approximation imposes that the dependence of the elastic T-matrix on the off-shell energy of the particle from which the photon is emitted is neglected. This amounts to omitting the retardation effects. It was shown by Martinus *et al.* [52] that this introduces uncertainties of at

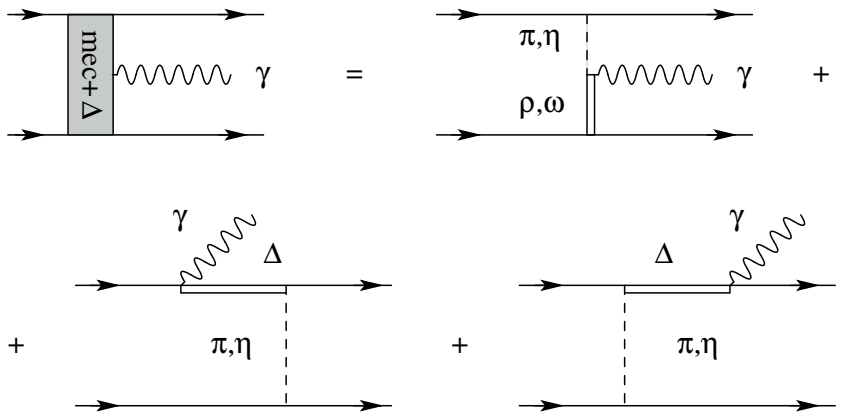

Figure 2.2: The Born terms of the two-body current bremsstrahlung. The first one is a MEC contribution, the other two are contributions of the Δ isobar.

most 10% at 280 MeV. For the case of the KVI experiment at 190 MeV, the effects are even smaller. In more detail, the expression for one of the IA contributions (final-state emission from leg 1) is

$$\langle f|J_\mu^{(IA)}|i\rangle \quad = \quad \langle p_1', p_2'|\Gamma_\mu^{(1)}(q)\, S^{(1)}(p_1'+q)\, T(\hat{p}_1'+\hat{q}, \hat{p}_2'; p_1, p_2)|p_1, p_2\rangle\,, \qquad (2.2)$$

where the hat over some momenta labeling the elastic T matrix means that in the center of mass of the nucleons their zeroth component will be set equal to zero.

The last term in Eq. (2.1) is the rescattering contribution to bremsstrahlung (see Fig. (2.1)). The four-dimensional integral appearing here is easily reduced to a three-dimensional one [52, 65, 66] since, as a result of the equal-time approximation, the elastic T matrix appearing in the integrand does not depend on the relative energy of the two nucleons, k_0. The k_0 integral for the rescattering diagram (the photon being emitted by the particle labeled i) is then of the form

$$I_0^{(i)} = \int \frac{d\,k_0}{2\pi}\, S^{(i)}(k_0, \vec{k}-\vec{q}; E')\, \Gamma_\mu^{(i)}(q)\, S_2(k_0, \vec{k}; E)\,, \qquad (2.3)$$

with $(\omega, \vec{q})$ the photon four-momentum, and can easily be evaluated analytically. The two-particle free propagator has been denoted by $S_2(k_0, \vec{k}; E)$. This is consistent with the equal-time framework used for treating the elastic NN problem.

In addition, contributions from the two-body currents, depicted in Fig. (2.2), have been considered. They include contributions from the meson-exchange currents (MEC) and the Δ isobar. In the Martinus *et al.* model for bremsstrahlung the two-body currents have been included in a perturbative way. Besides the Born term, single- and double-scattering contributions have been considered. The current operator for contributions from meson exchange currents (MEC) and the Δ isobar has the following expression in

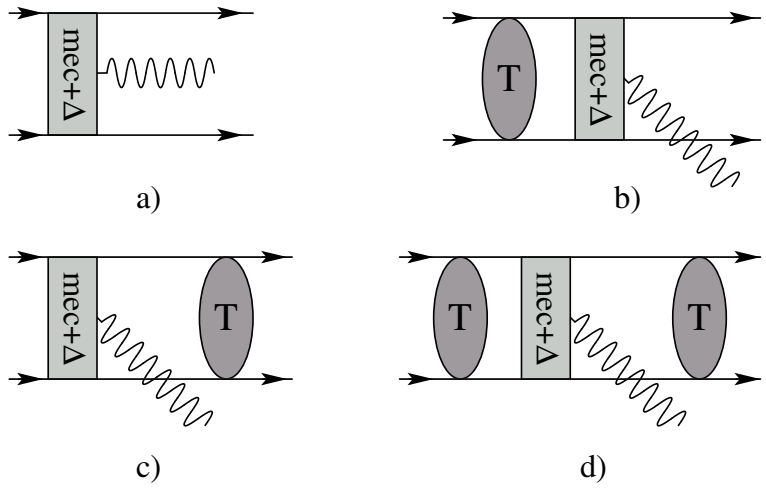

Figure 2.3: Two-body contributions to the bremsstrahlung amplitude. Diagram (a) represents the Born contribution, diagrams (b) and (c) single scattering terms and (d) is the rescattering contribution.

the center of mass of the incoming nucleons,

$$J_\mu^{MEC+\Delta} = \int\int \frac{d^4k'}{(2\pi)^4}\frac{d^4k}{(2\pi)^4} U(\Lambda)\overline{\Psi}(p',k';P')U^{-1}(\Lambda)\,(\Gamma_\mu^{MEC}+\Gamma_\mu^{\Delta})\Psi(k,p;P)\,, \quad (2.4)$$

where Λ denotes the Lorentz transformation from the center of mass (c.m.) system of the final nucleons to the c.m. of the initial nucleons, Γ_μ^{MEC} and Γ_μ^{Δ} represent the coupling of a photon to the NN system via MEC or a Δ isobar, and Ψ is a two-nucleon scattering state, given for the initial nucleons by

$$\Psi(p',p;P) = [(2\pi)^4\delta^4(p'-p) - iS_2(p',P)T(p',p;P)]|p,P\rangle\,, \quad (2.5)$$

where $|P\rangle$ is an antisymmetrized two-particle plane wave. In evaluating the four-dimensional integrals the BSLT approximation is again employed, and further, in performing the k_0 integration, only contributions from the intermediate nucleonic poles are retained. In the Martinus model the two-body contributions depicted in Fig. (2.3) are taken into account.

In the case of *pp* bremsstrahlung the leading-order meson-exchange contributions, the seagull and the pion-in-flight terms, vanish because in this case the exchanged particles are neutral. Therefore, the leading contributions come from decay type diagrams (Fig. (2.2)a). The coupling of mesons to nucleons is described identically as in the OBE model. The vertex of the decay of either of the vector mesons into the pion and photon is given by

$$\Gamma_{v\pi\gamma}^{\mu\nu} = -i\frac{eg_{v\pi\gamma}}{2m_v}\epsilon^{\mu\sigma\nu\tau}q_\sigma k_\tau^v\,, \quad (2.6)$$

with the values of the coupling constants $g_{\rho\pi\gamma}$=0.76 and $g_{\omega\pi\gamma}$=1.82 [66]. The uncertainties in these two coupling constants are of the order of 10-15%.

The leading contributions involving the Δ isobar are also decay type (Fig. (2.2)b,c). The πNΔ and ρNΔ vertices are taken to be of the form

$$\begin{aligned}\Gamma^{\mu}_{\pi N\Delta}(k) &= \frac{g_{\pi N\Delta}}{m_\pi}\Theta^{\mu\nu}(Z_\pi)k_\nu\,,\\ \Gamma^{\mu\nu}_{\rho N\Delta}(k) &= i\frac{g_{\rho N\Delta}}{m_\rho}[\not{k}\Theta^{\mu\nu}(Z_\rho)-\gamma^\mu k_\sigma\Theta^{\alpha\nu}(Z_\rho)]\gamma_5\,,\end{aligned} \tag{2.7}$$

with

$$\Theta^{\mu\nu}(Z)=g^{\mu\nu}-\Big(\frac{1}{2}+Z\Big)\gamma^\mu\gamma^\nu\,, \tag{2.8}$$

with $Z=1/2$ within the present model. The values of the coupling constants of the Δ-nucleon-meson vertices are given respectively by: $g^2_{\pi N\Delta}/4\pi$=0.35 and $g^2_{\rho N\Delta}/4\pi$=4.0 [66]. The $\gamma N\Delta$ vertex is given by

$$\begin{aligned}\Gamma^{\mu\nu}_{\gamma N\Delta}(p,q) &= -ie\Big(\frac{G_1}{M}\Theta^{\nu\alpha}(Z_1)\gamma^\beta+\frac{G_2}{M^2}\Theta^{\nu\alpha}(Z_2)p^\beta\Big)\\ &\quad\times(q^\alpha g^\nu_\beta-q_\beta g^\mu_\alpha)\gamma_5\,,\end{aligned} \tag{2.9}$$

with $G_1=2.51$ and $G_2=1.62$ and the off-shell parameters $Z_{1,2}$ were chosen equal to -1/2. The on-shell ($G_{1,2}$) and the off-shell ($Z_{1,2}$) parameters are sources of large uncertainties.

For the case of pp bremsstrahlung the $NN\gamma$ vertex is taken to be

$$\Gamma^{(i)}_\mu(q)=e(\gamma^{(i)}_\mu-\frac{i\kappa}{2M}\sigma^{(i)}_{\mu\nu}q^\nu) \tag{2.10}$$

where e is the proton electric charge and κ=1.79 is the anomalous magnetic moment of the proton.

2.2 Other models

In the next section numerical results of the Martinus $pp\gamma$ model will be presented. For comparison purposes we also present numerical results of two other models: the $pp\gamma$ model of Hermann, de Jong and Nakayama [49, 64, 67, 68] and a soft-photon model developed by Korchin and Scholten [60, 69]. To make comparison more transparent the relevant ingredients of these two models will be presented here.

2.2.1 Nakayama *et al.* model

The nucleonic current of the Nakayama *et al.* model for bremsstrahlung [49] consists of the same ingredients as the already discussed model of Martinus. For the elastic interaction the relativistic Bonn potential is used [14] and furthermore in the intermediate states the fermion propagator is chosen consistently with the one used for the solution of the elastic scattering problem [49]. The electromagnetic transition operator is split into four

contributions: convection, magnetic, relativistic spin corrections (RSC) and remaining relativistic corrections. The last one gives a negligible effect at intermediate nucleon energies. The first two terms have been traditionally used as the sole contributions to the electromagnetic current in early non-relativistic bremsstrahlung calculations. The RSC contributions are shown to lead to a decrease of the cross-section of the order 20-30% for proton angles larger than 15°. For the same kinematics the rescattering contribution leads to an increase of comparable magnitude leading to an almost perfect cancellation of the RSC and rescattering contributions. At small proton angles, of interest in this thesis, a similar cancellation does not take place, and a full relativistic calculation is therefore required. The model has been compared with the *unrenormalized* TRIUMF data [48] which are under predicted for most kinematics [49]. An inclusion of the much debated 2/3 normalization factor [48] would bring this model and the TRIUMF data in good agreement.

In Ref. [68] contributions from meson-exchange currents have also been considered. Only the $\omega\pi\gamma$ decay diagrams have been considered (they dominate over the ρ meson decay diagrams). They have been included at Born and single scattering level, *i.e.* the diagrams depicted in Fig. (2.3a,b,c). The value $g_{\omega\pi\gamma}$=3.53 has been used for the coupling constant. Contributions of the Δ isobar have been considered above the pion production threshold within a coupled-channel formalism which allows the Δ degrees of freedom [64, 68]. At 280 MeV the meson exchange diagrams contributions are about 1/3 from the Δ isobar contributions [68]. For the kinematics of the TRIUMF experiment the latter can give an increase of the cross-section up to 30% which brings the *unrenormalized* data and theory closer.

2.2.2 Soft-photon models

The soft-photon theorem for bremsstrahlung has been derived long time ago by Low [79, 80]. It states that the first two terms in a series expansion of the bremsstrahlung amplitude in terms of the frequency of the emitted photon depend only on parameters measurable in elastic nucleon-nucleon scattering and on static electromagnetic properties of the nucleon. Following this results soft-photon models for $NN\gamma$ have been developed [89, 90, 91] to name just a few of the elder ones. In the following the derivation of the original Low soft-photon amplitude [80] will be sketched.

We consider the scattering of two spin-1/2 particles. The fermion lines will be labeled 1 and 2 and the initial and final momenta of fermion i will be labeled with p_i and p_i' respectively. Both fermions have the same mass M and the momentum of the outgoing photon will be denoted by q. It will suffice to consider bremsstrahlung emission only from one of the nucleons, say nucleon 1, since the amplitude for the emission from nucleon 2 can be easily obtained by interchanging the variables referring to nucleon 1 with the ones referring to nucleon 2. The amplitude for bremsstrahlung emission can be split into an external and an internal part

$$M_\mu \quad = \quad M_\mu^{ext} + M_\mu^{int} \, . \tag{2.11}$$

The expression for the first is derived in a straightforward manner

$$\begin{aligned} M_\mu^{ext} &= \bar{u}(p_1')\Big[e\Big(\gamma_\mu + \frac{i\kappa}{2M}\sigma_{\mu\nu}q^\nu\Big)\frac{\not{p}_1' + \not{q} + M}{2p_1'\cdot q}\, T(p_1'+q, p_2'; p_1, p_2) \\ &\quad - T(p_1', p_2'; p_1 - q, p_2)\frac{\not{p}_1 - \not{q} + M}{2p_1\cdot q}\, e\Big(\gamma_\mu + \frac{i\kappa}{2M}\sigma_{\mu\nu}q^\nu\Big)\Big] u(p_1)\,. \end{aligned} \tag{2.12}$$

The elastic T matrix appearing in the above expression is evaluated at an half off-shell point. To arrive at the soft-photon expression for the amplitude an expansion in terms of the photon four-momentum q has to be performed. Before doing that the parametrization of the elastic T matrix has to be discussed. For the scattering of two spin-1/2 particles it can be put in the form [92, 93]

$$\begin{aligned} T(p_1', p_2'; p_1, p_2) &= \sum_{\alpha=1}^{5} F_\alpha\, G_\alpha\,, \\ G_\alpha &= \bar{u}(p_1')\,\lambda_\alpha\, u(p_1)\;\bar{u}(p_2')\,\lambda^\alpha\, u(p_2)\,, \\ \lambda_\alpha &= (1, \gamma_5, \gamma_\mu, \gamma_5\gamma_\mu, \sigma_{\mu\nu})\,, \end{aligned} \tag{2.13}$$

with F_α invariant functions of a complete set of Lorentz invariants). To keep expressions as clear as possible we will restrict the presentation to α=1, *i.e.* $T(p_1', p_2'; p_1, p_2) \equiv F_1(s,t,u)$. The scalar functions F_α depend on Lorentz invariants formed out of the four momenta (two incoming and two outgoing) that characterize an elastic scattering T matrix of two particles. Taking into account the momentum conservation relation and the on-shell condition only two independent invariants can be build out of the four external momenta. We choose them to be the following [80]

$$\begin{aligned} \nu &= p_1\cdot p_2 + p_1'\cdot p_2'\,, \\ \Delta &= (p_1' - p_1)^2 + (p_2' - p_2)^2\,. \end{aligned} \tag{2.14}$$

This choice corresponds to choosing s and t as the independent set of variables; the elastic scattering amplitudes dependent implicitly also on the masses of the external particles which in the case of an off-shell T matrix become active degrees of freedom. This is the case of the bremsstrahlung amplitude Eq. (2.12) for which we have

$$\begin{aligned} T(p_1'+q, p_2'; p_1, p_2) &= T(M_f^2, M^2; \nu_f, \Delta_f)\,, \\ T(p_1', p_2'; p_1 - q, p_2) &= T(M^2, M_i^2; \nu_i, \Delta_i)\,, \end{aligned} \tag{2.15}$$

where the following notations have been used

$$\begin{aligned} M_f^2 &= (p_1'+q)^2 = M^2 + 2p_1'\cdot q\,, \\ M_i^2 &= (p_1 - q)^2 = M^2 - 2p_1\cdot q\,, \\ \nu_f &= \nu + p_2'\cdot q\,, \\ \nu_i &= \nu - p_2\cdot q\,, \\ \Delta_f &= \Delta + 2q\cdot(p_1' - p_1)\,, \\ \Delta_i &= \Delta + 2q\cdot(p_1' - p_1)\,. \end{aligned} \tag{2.16}$$

Where possible the relation $q^2 = 0$ has been used, since we are dealing with real photons. Now, the elastic T matrices that enter the expression of external bremsstrahlung emission are expanded in Taylor series in the neighborhood of the on-shell point (ν, Δ). The following expressions are obtained

$$\begin{aligned} T(M_f^2, M^2, \nu_f, \Delta_f) &= T(\nu,\Delta) + 2p_1' \cdot q \, \frac{\partial T}{\partial M_f^2} + p_2' \cdot q \, \frac{\partial T}{\partial \nu} + 2q \cdot (p_1' - p_1) \, \frac{\partial T}{\partial \Delta} \,, \\ T(M, M_i^2, \nu_i, \Delta_i) &= T(\nu,\Delta) + 2p_1 \cdot q \, \frac{\partial T}{\partial M_i^2} - p_2 \cdot q \, \frac{\partial T}{\partial \nu} + 2q \cdot (p_1' - p_1) \, \frac{\partial T}{\partial \Delta} \,, \\ T(\nu,\Delta) &\equiv T(M^2, M^2; \nu, \Delta) \,. \end{aligned} \tag{2.17}$$

All the derivatives of the elastic T matrix are evaluated at the on-shell point, even tough this is not explicitly shown. The requirement of gauge invariance of the whole amplitude

$$q^\mu M_\mu^{ext} + q^\mu M_\mu^{int} \equiv 0 \,, \tag{2.18}$$

allows the determination, up to individually gauge invariant terms, of the internal bremsstrahlung amplitude M_μ^{int}. In the construction of the soft-photon amplitude only term proportional with $1/k$ and k^0 are kept, in accordance with the soft-photon theorem. Employing such a procedure results in the following expression for the internal bremsstrahlung amplitude

$$M_\mu^{int} = \bar{u}(p_1') \, e \left[2p_{1\,\mu}' \, \frac{\partial T}{\partial M_f^2} - 2p_{1\,\mu} \, \frac{\partial T}{\partial M_i^2} + (p_2 + p_2')_\mu \, \frac{\partial T}{\partial \nu} \right]. \tag{2.19}$$

In the process of derivation of this expression, Dirac's equation and the anticommutation relation of the γ matrices were used. Adding to it the expression of the external bremsstrahlung, Eq. (2.12), results in the final expression for bremsstrahlung emission

$$\begin{aligned} M_\mu = e\bar{u}(p_1') \Bigg[& \Big(\frac{p_{1\,\mu}'}{p_1' \cdot q} \, T(\nu,\Delta) - T(\nu,\Delta) \, \frac{p_{1\,\mu}}{p_1 \cdot q} \Big) \\ & + \Big(\frac{\gamma_\mu \not{q}}{2p_1' \cdot q} \, T(\nu,\Delta) + T(\nu,\Delta) \, \frac{\not{q} \gamma_\mu}{2p_1 \cdot q} \Big) \\ & + \frac{i\kappa}{2M} \sigma_{\mu\nu} q^\nu \, \frac{\not{p}_1' + M}{2p_1' \cdot q} \, T(\nu,\Delta) - T(\nu,\Delta) \, \frac{\not{p}_1 + M}{2p_1 \cdot q} \, \frac{i\kappa}{2M} \sigma_{\mu\nu} q^\nu \\ & + \Big(\frac{p_2' \cdot q}{p_1' \cdot q} \, p_{1\,\mu}' + \frac{p_2 \cdot q}{p_1 \cdot q} \, p_{1\,\mu} - p_{2\,\mu}' - p_{2\,\mu} \Big) \, \frac{\partial T}{\partial \nu} \\ & + q \cdot (p_1' - p_1) \Big(\frac{p_{1\,\mu}'}{p_1' \cdot q} - \frac{p_{1\,\mu}}{p_1 \cdot q} \Big) \, \frac{\partial T}{\partial \Delta} \Bigg] u(p_1) + \mathcal{O}(k) \,. \end{aligned} \tag{2.20}$$

In the final result the derivatives in the off-shell direction (with respect to M_f^2 or M_i^2) have disappeared, due to a cancellation of the respective terms from the external and internal contribution expressions against each other. This is the content of the soft-photon theorem. Eq. (2.20) is the form of the soft-photon amplitude, as derived by Low in Ref. [80]. The soft-photon theorem has been extended and generalized later by many

authors and many soft-photon amplitudes have been constructed using the standard Low procedure.

The standard Low procedure has two obvious short-comings: it does not allow one to obtain an internal contribution which is separately gauge invariant and it cannot be applied in regions where the elastic amplitude varies rapidly as a function of energy and/or scattering angle because in that case the Taylor expansion Eq. (2.17) would fail. In order to solve these issues a generalized soft-photon amplitude, obtained via a modified Low procedure, has been proposed [94, 95]. Its construction is obtained in two steps [95]: first a tree-level amplitude $\bar{M}_\mu$ is derived, which is the sum of external tree-level emission diagrams ($\bar{M}_\mu^E$), emission from dominant tree-level internal lines ($\bar{M}_\mu^I$) and a term derived from imposing gauge invariance ($\bar{M}_\mu^G$). Then, the general amplitude M_μ is derived as the sum of general external emission diagrams (the same procedure as the standard Low), general internal lines emission which reduce to ($\bar{M}_\mu^I$) at tree-level approximation and a third term obtained from gauge invariance. The first two terms of the expansion of the general amplitude in terms of the photon four-momentum define the general soft-photon amplitude. The expansion of M_μ is performed in such a way that the expanded M_μ depends on the elastic T matrix evaluated at some on-shell point, but it is free of derivatives with respect of the specified Mandelstam variables which alleviates the second mentioned problem of the Low soft-photon amplitude. Together with the generalization of the original *st* Low amplitude, a new class of soft-photon amplitudes (*ut*) has been developed [95]. In Ref. [59] it has been shown that an amplitude from the *ut* class, the special two-u-two-t (TsTts), can be used to describe $pp\gamma$ experimental data for kinematics for which the original Low amplitude fails. In Ref. [93] the incorporation of the Pauli principle was realized for the TuTts amplitude while for the *st* class of amplitudes it was shown that a similar result was not possible leading to a serious violation.

In Refs. [60, 69] Korchin and Scholten have developed two soft photon amplitudes for virtual nucleon-nucleon bremsstrahlung by using the standard Low approach and the modified Low approach of Ref. [59, 95] respectively. The Pauli principle was incorporated as well as crossing symmetry. In the limiting case when the mass of the virtual photon goes to zero, their models can be applied to real nucleon-nucleon bremsstrahlung.

2.3 Comparison with the experimental KVI data

A comparison of the Martinus $pp\gamma$ model with the TRIUMF data has been presented elsewhere [52, 63]. The predicted cross-sections lie systematically below the TRIUMF data [48], the difference being of the order of 10-15%. The discrepancy can be alleviated once the normalization factor of 2/3 is taken into account. At T_{lab}=280 MeV sizable contributions of the Δ isobar are predicted (the θ_1=12°, θ_2=27.8° and θ_1=28°, θ_2=27.8° kinematics), up to 50-60%, while the contributions of the meson-exchange currents are generally small. These features are in good agreement with the results of the Nakayama *et al.* model.

More recently, a $pp\gamma$ experiment has been performed at KVI [57, 58, 81] at an incoming proton energy of 190 MeV. Cross sections and analyzing powers have been measured with an unprecedented accuracy. A later reanalysis of the experimental data has yielded

improved results for the analyzing powers [82] while the original reported [57] values of the cross-sections have remained unchanged. We present here a comparison of the $pp\gamma$ models described in this chapter with a small, but representative, selection of the KVI proton-proton bremsstrahlung experimental data. It has already noted some time ago [58] that microscopic models fail to reproduce an important fraction of the KVI experimental data, while for others the agreement is fairly good. We have selected 6 kinematics for which results are presented. In Fig. (2.4) kinematics for which the azimuthal angle of the photon, θ_γ, is varied are displayed. In a second plot, Fig. (2.5), kinematics for which one of the angles of the outgoing protons (θ_1 or θ_2) is varied are shown. All the cases presented here correspond to coplanar kinematics, with the emitted photon being on the same side of the incoming beam as the outgoing proton labeled 1. Besides the predictions of the Martinus $pp\gamma$ model, results of the microscopic model of Nakayama [96] and of the soft-photon calculation of Korchin and Scholten [97] are presented. Experimental data taken during the KVI experiment with two setup configurations, BLOCK (triangles) and SUPERCLUSTER (squares) [58], are shown.

From the two shown figures one observes that the microscopical calculations of Martinus and Nakayama yield close results to each other for all of the kinematical situations presented. The calculation of Nakayama *et al.* (dotted line) below the pion production threshold does not incorporate the contributions of the Δ isobar. A direct comparison with the full Martinus model (full line) is therefore not completely justified. The similarities between the two have to do with the fact that for $pp\gamma$ at 190 MeV meson-exchange and the Δ isobar contributions only give rise to almost negligible effects (compare the full and dashed curves), visible in Fig. (2.4) and Fig. (2.5) as an approximately uniform background over the phase-space. The contributions of the two-body currents become relatively more important towards the regions of minimum for the cross-section, where their contributions are important for a proper description of the experimental data (see for example the θ_1=8°, θ_2=16° kinematics in Fig. (2.4) in the region θ_γ=90°).

A second easily observable feature is a large discrepancy between the Martinus and Nakayama models on one side and the experimental KVI data on the other side for specific kinematics. The discrepancy occurs at the peaks of the cross-section of four of the kinematical cases presented here: θ_1=8° - θ_2=16°, θ_1=8° - θ_2=19°, θ_2=16° - θ_γ=145° and θ_1=8° - θ_γ=145°. The same holds true for other microscopical $pp\gamma$ models, when compared with the KVI experimental data, too [58]: the model of Gari and Eden [51, 98] overshoots the mentioned experimental data at the peaks by even larger amounts. The predictions for the analyzing power A_y of both microscopical models are reasonably close to the experiment, but for this observable the experimental results are not as accurate as for the differential cross-section.

A different situation exists in the case of the soft-photon calculation. Their predictions are in a satisfactory agreement with the experimental data for all the presented kinematics. Both the *ut* and *st* class models predict similar results for both the cross-sections and analyzing powers. A well known feature of soft-photon models, the inability to properly reproduce the experimental analyzing powers, is observed here as well.

The sources for the observed discrepancy between the microscopical model of Martinus and KVI experimental data are the object of study in the next two chapters. Two possible sources of the discrepancy have been studied: Coulomb effects due to the well-

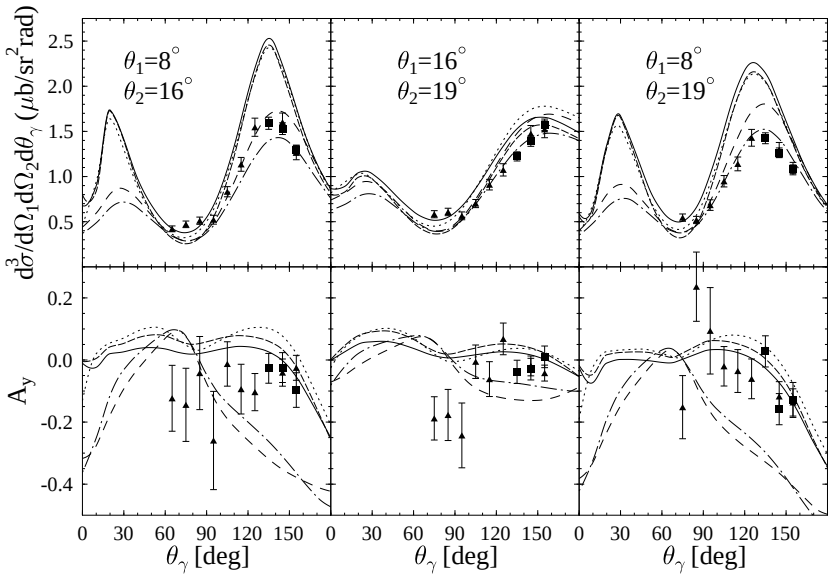

Figure 2.4: Cross-sections and analyzing powers for pp bremsstrahlung at T_{lab}=190 MeV. The experimental point (squares and circles) are the result of the KVI $pp\gamma$ experiment. Martinus model predictions are given by the full (full model) and dashed (only nucleonic contributions) lines; the dotted curve denotes the model of Nakayama; soft-photon model results of Korchin and Scholten are plotted using dashed-dotted (ut) and short-dashed (st) lines.

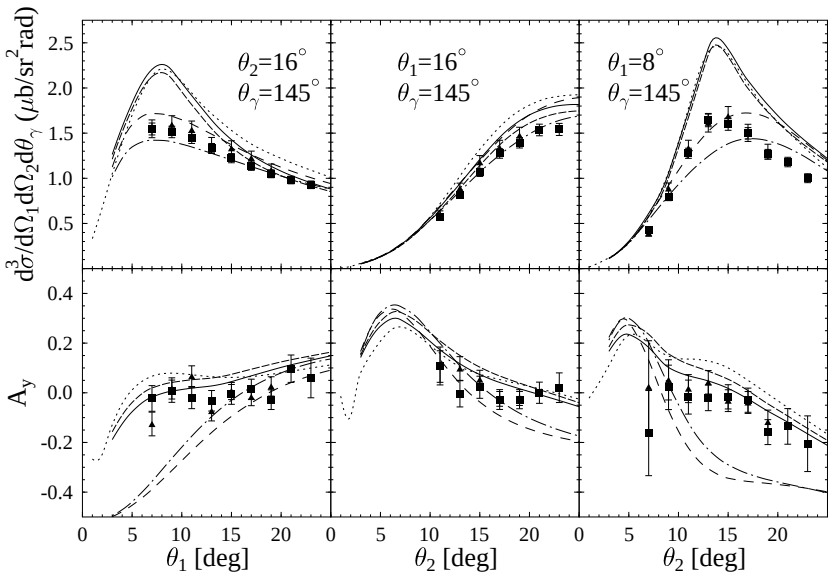

Figure 2.5: The same as Fig. (2.4) but for different kinematics.

known repulsion between two equally electrically charged particles and sensitivity of the bremsstrahlung cross-section to the on-shell nucleon-nucleon interaction.